Hydroclimate of the western Indo-Pacific Warm Pool during the past 24,000 years

Eva M. Niedermeyer[a,b,1], Alex L. Sessions[a], Sarah J. Feakins[c], and Mahyar Mohtadi[d]

[a]Division of Geological and Planetary Sciences, California Institute of Technology, Pasadena, CA 91125; [b]Biodiversity and Climate Research Centre (BiK-F) and Senckenberg Gesellschaft für Naturforschung, D-60325 Frankfurt, Germany; [c]Department of Earth Sciences, University of Southern California, Los Angeles, CA 90089; and [d]MARUM–Center for Marine Environmental Sciences, University of Bremen, D-28359 Bremen, Germany

Edited by Thure E. Cerling, University of Utah, Salt Lake City, UT, and approved May 6, 2014 (received for review January 13, 2014)

The Indo-Pacific Warm Pool (IPWP) is a key site for the global hydrologic cycle, and modern observations indicate that both the Indian Ocean Zonal Mode (IOZM) and the El Niño Southern Oscillation exert strong influence on its regional hydrologic characteristics. Detailed insight into the natural range of IPWP dynamics and underlying climate mechanisms is, however, limited by the spatial and temporal coverage of climate data. In particular, long-term (multimillennial) precipitation patterns of the western IPWP, a key location for IOZM dynamics, are poorly understood. To help rectify this, we have reconstructed rainfall changes over Northwest Sumatra (western IPWP, Indian Ocean) throughout the past 24,000 y based on the stable hydrogen and carbon isotopic compositions (δD and $\delta^{13}C$, respectively) of terrestrial plant waxes. As a general feature of western IPWP hydrology, our data suggest similar rainfall amounts during the Last Glacial Maximum and the Holocene, contradicting previous claims that precipitation increased across the IPWP in response to deglacial changes in sea level and/or the position of the Intertropical Convergence Zone. We attribute this discrepancy to regional differences in topography and different responses to glacioeustatically forced changes in coastline position within the continental IPWP. During the Holocene, our data indicate considerable variations in rainfall amount. Comparison of our isotope time series to paleoclimate records from the Indian Ocean realm reveals previously unrecognized fluctuations of the Indian Ocean precipitation dipole during the Holocene, indicating that oscillations of the IOZM mean state have been a constituent of western IPWP rainfall over the past ten thousand years.

plant wax δD | plant wax $\delta^{13}C$ | Indonesia

The Maritime Continent (~10°S–20°N and 90°E–130°E) is situated within the Indo-Pacific Warm Pool (IPWP). Here, intense atmospheric convection and rainfall provide a major driving force for global atmospheric circulation. On a seasonal basis, regional hydrology is governed by migration of the Intertropical Convergence Zone (ITCZ) and associated changes of the monsoonal wind flow. In addition, IPWP hydrology undergoes strong and abrupt variations on an interannual scale that have been linked to the El Niño Southern Oscillation (ENSO), and more recently to the coupled atmosphere-ocean system over the Indian Ocean (Indian Ocean Zonal Mode, IOZM) (1, 2). Whereas ENSO has a significant impact on rainfall patterns across the eastern and southern areas of the Maritime Continent, there appears to be no direct impact of ENSO on rainfall patterns of Northwest (NW) Sumatra (3). Instead, fluctuations of the IOZM may exert substantial control on NW Sumatran rainfall variability (1). At present, annual mean rainfall received in the western IPWP (>3,000 mm) is higher than that in equatorial East Africa (about 500–700 mm; www.worldclim.org/), resulting in a precipitation dipole across the Indian Ocean. During years of so-called IOZM events, anomalous cooling (warming) off Sumatra (East Africa) corresponds to negative (positive) rainfall anomalies along western Sumatra (East Africa), resulting in a weakening or even reversal of the Indian Ocean precipitation gradient. A recent proxy data-modeling approach combining a set of relative moisture reconstructions from East Africa and simulations from coupled climate models suggests an IOZM-like relationship between eastern Indian Ocean cooling and positive rainfall anomalies in East Africa on decadal timescales during the past millennium (4). Coral-based reconstructions of sea surface temperature (SST) anomalies in the eastern tropical Indian Ocean (off the coast of West Sumatra) indicate distinct periods of IOZM variability throughout the past 7,000 y (5, 6). However, despite the pronounced impact of the IOZM on present-day hydrology of Indian Ocean rim countries (e.g., refs. 7 and 8), the importance of the Indian Ocean for past rainfall variability over the western IPWP has not yet been demonstrated.

To help fill this gap, we explored precipitation changes in NW Sumatra during the past 24,000 y recorded in a marine sediment core from the Nias basin (yellow star in Fig. 1; eastern Indian Ocean). The study site is under the influence of modern sea surface anomalies associated with IOZM variability, making it an ideal location to study past variability of the Indian Ocean precipitation gradient.

At present, the study site receives abundant rainfall carried by tropical maritime trade winds throughout the year with no dry season (9). Local rainfall amounts are largely independent of the seasonal migration of the ITCZ as the site remains within the tropical rain belt year-round (for a detailed description of moisture supply over the Maritime Continent, see *SI Text* and Figs. S1 and S2). Present-day rainfall anomalies are modulated by SST anomalies relating to the IOZM (1). There appears to be

Significance

The Indo-Pacific Warm Pool (IPWP) is the largest source of atmospheric water vapor, and region of highest rainfall, on Earth. At irregular intervals, this high-rainfall regime weakens, causing severe droughts with massive consequences for the local population. Research into the underlying mechanisms is limited by the temporal coverage of climate data. We produced a record of rainfall over the western IPWP covering the past 24,000 years. Our data indicate that topography and coastline position govern regional IPWP hydrology on glacial–interglacial timescales. During the Holocene, western IPWP rainfall is linked to that of East Africa through a precipitation dipole. Fluctuations of this dipole identified in our study serve as an impetus for future studies to advance our understanding of IPWP dynamics.

Author contributions: E.M.N., A.L.S., and M.M. designed research; E.M.N. performed research; A.L.S., S.J.F., and M.M. contributed new reagents/analytic tools; E.M.N. analyzed data; E.M.N. wrote the paper.

The authors declare no conflict of interest.

This article is a PNAS Direct Submission.

[1]To whom correspondence should be addressed. E-mail: eva.niedermeyer@senckenberg.de.

This article contains supporting information online at www.pnas.org/lookup/suppl/doi:10.1073/pnas.1323585111/-/DCSupplemental.

no direct influence of ENSO on precipitation in NW Sumatra (3); however, an indirect impact of ENSO is observed during periods of ENSO and IOZM event interactions (10).

We measured the stable hydrogen (δD) and stable carbon ($\delta^{13}C$) isotopic composition of terrestrial plant waxes, specifically the n-C_{30} and n-C_{32} alkanoic acids, to deduce changes of hydrology and vegetation on land. We infer that higher plant waxes deposited at the study site predominantly derive from the adjacent hinterland of NW Sumatra, as the mineralogy and radiogenic composition of clay minerals deposited offshore from the North Sumatran Shelf indicate rocks of North and central Sumatra as the dominant source of terrestrial material (11, 12) (*SI Text*). Plant wax δD values have been shown to correlate with those of precipitation (13), which, in the tropics, relate to the amount of rainfall (14) (*SI Text*).

Since there is debate about whether photosynthetic pathway and plant morphology has an influence on the δD value of plant waxes (13), we also measured their $\delta^{13}C$ values during periods of pronounced changes in plant wax δD.

Results

The δD values of the n-C_{30} alkanoic acids (Fig. 2*A*) range from −148‰ to −175‰. We identify two periods of D depletion around 14 ka and 11.5 ka during the last glacial period as well as two pronounced periods of D depletion during the Holocene from about 8 ka to 6.5 ka and from 2 ka to 1 ka, and an interval of moderate D depletion lasting from about 4.5 ka to 2.5 ka. The temporal pattern of δD values of the n-C_{32} alkanoic-acid δD record (Fig. 2*B*) matches that of the n-C_{30} alkanoic acid during the Holocene, replicating the observed variability. Due to coelution of an unknown compound (*SI Text*), the n-C_{32} alkanoic acid record could not be extended to the Last Glacial Maximum (LGM).

Values of $\delta^{13}C$ (Fig. 2*C*) show little variation throughout the record (about 2‰ when corrected for glacial–interglacial changes in atmospheric $^{13}CO_2$; see *SI Text*), indicating persistent dominance of C_3 plants throughout the study interval. This agrees with palynological studies from the highlands of NW Sumatra from Lake Toba (15), and central Sumatra at Danau Padang (16) and Danau di Atas (17), which demonstrate that tropical trees (which are C_3 plants) persisted throughout the time interval covered by our record. We therefore have no evidence for changes in vegetation that might have influenced the δD values of plant waxes at the study site.

Discussion

We account for changes in the δD value of rainfall due to deglaciation by correcting our record for glacial–interglacial changes of ice volume and temperature. Our temperature correction (*SI Text* and Fig. S3) includes the minimum and maximum estimates of local glacial–interglacial temperature differences of about 3 °C for the marine realm (18, 19) and of up to 7 °C on land (20). The combined effects of ice volume [~1‰ $\delta^{18}O$ seawater (21) accounting for an −8‰ D depletion during the LGM] and surface temperature change [which accounts for a D enrichment during the LGM of +2.4‰ to +5.6‰ (22)] act on the δD signal in opposite directions, yielding a net isotopic depletion of −2.5‰ to −5.5‰ during the LGM (Fig. 2*A*). Assuming no contribution of D-depleted vapor from the exposed Sunda Shelf [continental effect (14)], we attribute the remaining variability of the δD record to changes in the amount of rainfall received in the study area, with periods of D depletion corresponding to intervals of enhanced rainfall amounts and vice versa.

No Trend in LGM to Holocene Patterns in Rainfall. Both the corrected and uncorrected n-C_{30} alkanoic acid δD records reveal no apparent glacial–interglacial difference in the amount of rainfall received at the study site (Fig. 2*A*). Instead, average rainfall amounts in NW Sumatra were of about the same order of magnitude or slightly elevated during the LGM compared with the Holocene, depending on the true impact of temperature change on the δD values of our record. This observation is in agreement with reconstructions of seawater $\delta^{18}O$ off West Sumatra (19) displaying similar values during the LGM and the Holocene, and is further supported by palynological evidence from central West Sumatra indicating cooler but not drier conditions during the LGM (summarized in ref. 23).

The lack of drying in West Sumatra during the LGM contrasts with evidence for concurrent drying across the central IPWP. Reconstructions of glacial–interglacial changes in terrestrial precipitation based on speleothem calcite $\delta^{18}O$ records from Borneo (24) and Flores (25), and a plant wax δD record from Sulawesi (26), indicate drier than present conditions during the LGM [Borneo (24)] followed by an increase of precipitation during deglaciation [Flores, Sulawesi (25, 26)] (Fig. 2 *E*–*G*).

We suggest that these distinctive differences between the eastern and western Maritime Continent result from exposure of the Sunda Shelf during the LGM and resulting changes in regional ocean and atmosphere circulation. During the LGM, when the Sunda Shelf was exposed (27), the study sites of Borneo, Flores, and Sulawesi were connected to a more continental geography, whereas NW Sumatra experienced only a minor change in coastline position (Fig. 1*A*). According to Griffiths et al. (25), the glacioeustatically forced flooding of Sundaland during the last deglaciation increased the surface area of ocean water along the monsoon trajectory delivering moisture to the southern and eastern Maritime Continent, enhancing rainfall amounts across the central IPWP. Precipitation over the western IPWP (West Sumatra), however, derives almost exclusively from the Indian Ocean and is orographically shielded from that in the central IPWP through the Barisan Mountain rise (28, 29). Rainfall in equatorial West Sumatra is dominantly generated

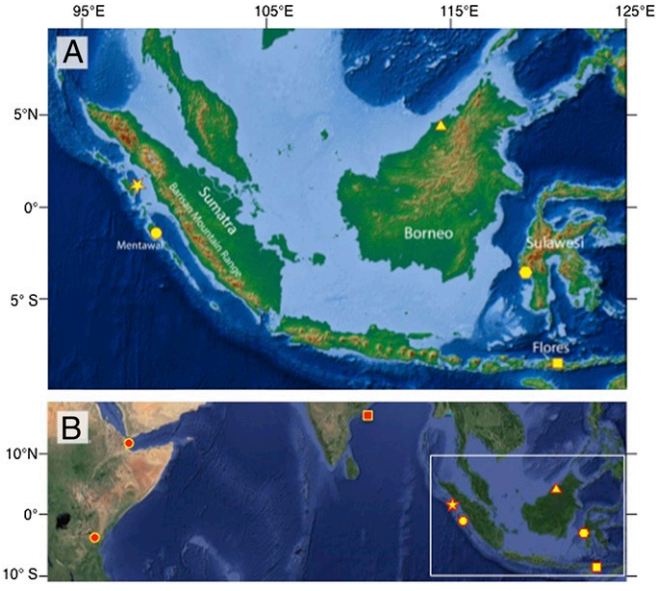

Fig. 1. (*A*) Topography and bathymetry of the Maritime Continent and the surrounding ocean. Note that color coding refers to topography/bathymetry only; brown areas do not indicate absence of vegetation. Lightest blue shading indicates the shallow shelf up to 120 m below sea level. Yellow symbols indicate IPWP study sites: this study (star), Mentawai islands (6) (circle), Flores (25) (rectangle), Sulawesi (26) (hexagon), and Borneo (24) (triangle). (*B*) Additional study sites cited in the manuscript in East Africa (34, 35) (red circles) and Southeast India (37) (red square). Map used by permission, Copyright © 2014 Esri. All rights reserved.

through convection and orographic uplift of moist air along the western Barisan Mountain Range, whereas the leeward East of Sumatra receives additional moisture from the central Pacific. In this way, it is reasonable to expect that the LGM-to-Holocene hydrological development of West Sumatra differed from that of Borneo, Flores, and Sulawesi, illustrating the importance of orography and land–sea distribution for IPWP climate during the LGM.

A more northerly position of the ITCZ during the mid-Holocene resulted in a strengthening of the Southeast monsoon (18, 23, 30) at the study site, but was not accompanied by changes in the amount of local rainfall in NW Sumatra (Fig. 2*A*). At present, the amount of rainfall received in tropical, NW Sumatra is largely independent of ITCZ position (3, 9), and, unlike at Borneo, Flores, and Sulawesi, seasonal changes of moisture sources do not display seasonal cycles in rainwater δD (*SI Text* and Fig. S1). Our data suggest that this pattern has persisted throughout the past 24 ka.

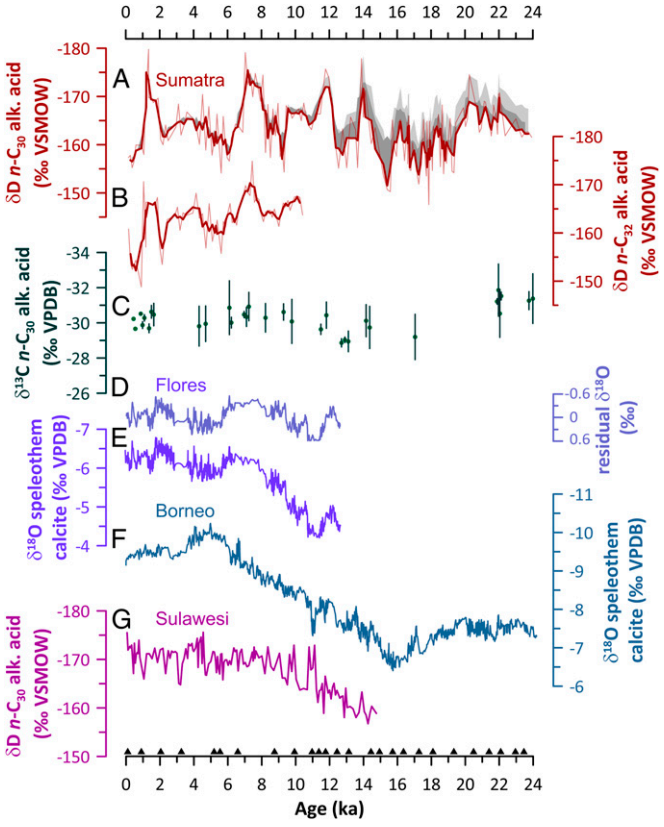

Fig. 2. δD Records of n-C_{30} and n-C_{32} alkanoic acids (this study) together with stable isotope records from the Maritime Continent (IPWP). (*A*) Median δD values of the n-C_{30} alkanoic acid plotted as original values (thin red line) and three-point running mean (thick red line). Shaded areas indicate corrections made for the combined effects of glacial–interglacial changes in ice volume and temperature changes of 3 °C (light gray) and 7 °C (dark gray). For details regarding the correction, see *SI Text* and Fig. S3. (*B*) δD values of the n-C_{32} alkanoic acid as in *A*. (*C*) Median $\delta^{13}C$ values of the n-C_{30} alkanoic acid (not corrected for glacial–interglacial changes in atmospheric $^{13}CO_2$) with 1σ error bars. (*D*) $\delta^{18}O$ of speleothem calcite from Flores (25) after detrending to reveal precipitation changes in southern IPWP rainfall other than those induced by sea level rise. (*E* and *F*) Three-point running average of speleothem-calcite $\delta^{18}O$ values from (*E*) Flores (25) and (*F*) Borneo (24), both plotted on axes that are scaled to match the amplitude of δD variability (by factor of 8) in *A* and *B*. (*G*) The n-C_{30} alkanoic-acid δD values from Sulawesi [ice volume corrected (26)]. Black triangles indicate ^{14}C age control points of core SO189-144KL (38). VPDB, Vienna Pee Dee Belemnite; VSMOW, Vienna standard mean ocean water.

Millennial-Scale Changes in Rainfall Variability. Changes in the amount of precipitation recorded in the western IPWP are characterized by millennial-scale variability. During the last deglacial, the Sumatra δD record (Fig. 2*A*) displays an interval of elevated rainfall amounts between about 14.6 ka and 13.8 ka that may relate to the Bølling–Allerød, whereas precipitation amounts during the Younger Dryas period (~12.8–11.5 ka) are ambiguous, changing significantly during the middle of this interval.

Interestingly, precipitation in NW Sumatra shows two distinct periods of high rainfall amounts during the Holocene from about 8 ka to 6.5 ka and from 2 ka to 1 ka (Fig. 2 *A* and *B*). An additional period of increased moisture is indicated between 4.5 ka and 2.5 ka (best seen in the δD record of the n-C_{32} alkanoic acid; Fig. 2*B*). These are striking features as these pronounced hydrological shifts occur during the relatively stable climate of the Holocene.

To explore whether this is a local or a more regional feature, we applied a 10-ka high-pass filter (31) to the isotope records from Borneo, Sulawesi, and Flores to reveal rainfall variability superimposed upon that attributable to the deglacial sea level rise. In particular, we examined whether or not the residual records display periods of isotope enrichment or depletion contemporary to the two distinct intervals of rainfall increase recorded at Sumatra from 8 ka to 6.5 ka and from 2 ka to 1 ka. Whereas the residuals from Borneo and Sulawesi (Fig. S4) display no such match, residual changes in the Flores $\delta^{18}O$ record (Fig. 2*D*) reveal similarities with Holocene changes of rainfall recorded at our study site regarding the sequence of deuterium and/or ^{18}O depletion and enrichment. Specifically, the interval of depletion from 8.5 ka to 6 ka recorded in Flores (about −0.5‰ in $\delta^{18}O$) coincides with an interval of enhanced rainfall in Sumatra [cross-correlation (32) $r = 0.6$; $P < 0.001$]. An additional interval of ^{18}O depletion in Flores is recorded from about 2.9 ka to 1.5 ka. Whether or not this relates to the period of elevated rainfall at Sumatra from 2 ka to 1 ka or to an interval of reduced precipitation around 2 ka, however, cannot be resolved at this point as the respective intervals in Flores and Sumatra overlap: Cross-correlation reveals no significant correlation, whereas shifting the residuals from Flores by 500 y results in a positive correlation of $r = 0.74$ ($P < 0.001$). Moreover, the residual variability recorded in Flores is generally less abrupt and of lower amplitude than that in Sumatra, possibly indicating a heterogeneous climate response to a potentially common climate forcing.

Fluctuations of the Indian Ocean Precipitation Dipole During the Holocene. The apparent insensitivity of NW Sumatran rainfall to both the last deglacial sea level rise and shifts of ITCZ position makes our study site a unique location to differentiate precipitation changes that may derive from changes of the IOZM. Yet as the last glacial is an interval with very different global climate boundary conditions compared to the present, we restrict the following discussion to precipitation changes and their possible link to the IOZM during the Holocene. At present, annual mean rainfall received in NW Sumatra is higher than that in tropical East Africa, and persistence of drought tolerant vegetation at Lake Challa (33) vs. tropical rainforest in NW Sumatra (this study) throughout the Holocene indicates that an East–West precipitation dipole has been a general characteristic of the Indian Ocean realm over the past 10 ka. We compared our plant wax δD record to rainfall reconstructions from East Africa and Southeast India, as well as to eastern Indian Ocean SST anomalies to explore Holocene characteristics of the IOZM (see Fig. 1*B* for locations of the study sites). We applied a 10-ka high-pass filter (31) to the paleo-precipitation

records from East Africa to reveal rainfall changes superimposed on long-term forcing patterns of the East African monsoon.

During the early Holocene, the Sumatran plant wax δD record displays an interval of elevated rainfall amounts from ~8 ka to 6.5 ka (Fig. 3*D*) whereas the filtered plant wax δD records from Lake Challa (34) and the Gulf of Aden (35) indicate reduced rainfall amounts in East Africa (Fig. 3 *A* and *B*), suggesting a strengthening of the Indian Ocean Precipitation Dipole during that interval. Interestingly, these rainfall excursions further overlap with an interval of positive sea surface anomalies in the eastern Indian Ocean as recorded in corals from the Mentawai Islands (6) (Fig. 3*E*). At present, anomalous warming (cooling) in the eastern (western) tropical Indian Ocean ["negative" ("positive") IOZM] results in wetter (drier) conditions along NW Sumatra (East Africa) (1, 2). A strengthened East–West precipitation dipole across the Indian Ocean together with warming in the eastern Indian Ocean as indicated by the paleoproxy records therefore suggests a shift of the IOZM toward a negative-event-like mean state in analogy to modern-day IOZM events.

The early Holocene rainfall peak in NW Sumatra is followed by a period of decreased rainfall amounts from about 6.5 ka to 4.5 ka together with elevated rainfall in East Africa as indicated at Lake Challa (Fig. 3*B*), suggesting a weakening of the Indian Ocean precipitation gradient. Hydrologic conditions recorded in the Gulf of Aden (Fig. 3*A*), however, are ambiguous during that interval. Yet, consistent with the above, concurrent cooling in the eastern Indian Ocean (Fig. 3*E*) suggests a shift of the IOZM toward a positive-event-like mean state during that interval. The extent to which this may have induced a reversal of the precipitation dipole remains unanswered as the δD records do not quantitatively reflect changes in rainfall amount.

The mid-Holocene warm SST anomaly offshore Sumatra around 4 ka (Fig. 3*E*), which is of the same order of magnitude as the one during the early Holocene, again coincides with a period of reduced rainfall amounts in East Africa (Fig. 3 *A* and *B*) but only a slight increase of precipitation in NW Sumatra (Fig. 3*D*). This may indicate a nonlinear relationship between eastern Indian Ocean SST anomalies and corresponding precipitation changes in the western IPWP, or that our study site was not located within the core of precipitation changes at the time. We note, however, that the mid-Holocene warming in the eastern Indian Ocean coincides with a shift of the zonal gradient of Pacific SSTs toward cooling in the eastern IPWP [i.e., toward El-Niño-like conditions (36)]. We suggest that such a weakened Pacific Walker circulation during this interval would have dampened the effect of eastern Indian Ocean SST warming at our study site, resulting in a more modest strengthening of eastern Indian Ocean Walker circulation and precipitation than one might expect from the magnitude of eastern Indian Ocean warming alone.

The most recent and distinct rainfall maximum recorded in NW Sumatra in the late Holocene from ~2 ka to 1 ka (Fig. 3*D*) coincides with a concise interval of reduced precipitation in East Africa (Fig. 3 *A* and *B*) and Southeast India (37) (Fig. 3*C*), providing strong evidence for a negative precipitation dipole across the Indian Ocean (i.e., higher rainfall amounts in the western IPWP) during that interval. Whether or not this relates to changes of Indian Ocean SST cannot be assessed in this study due to a gap in the Mentawai coral record. However, based on modern-day dynamics of the IOZM and associated rainfall patterns on the surrounding continents (1, 2), we surmise a positive (negative) SST anomaly in the eastern (western) Indian Ocean during that period. To what extent rainfall variability recorded in Southeast India consistently compares to either eastern or the western precipitation remains elusive due to the very different sampling resolutions of the plant wax records compared with the $\delta^{18}O$ record.

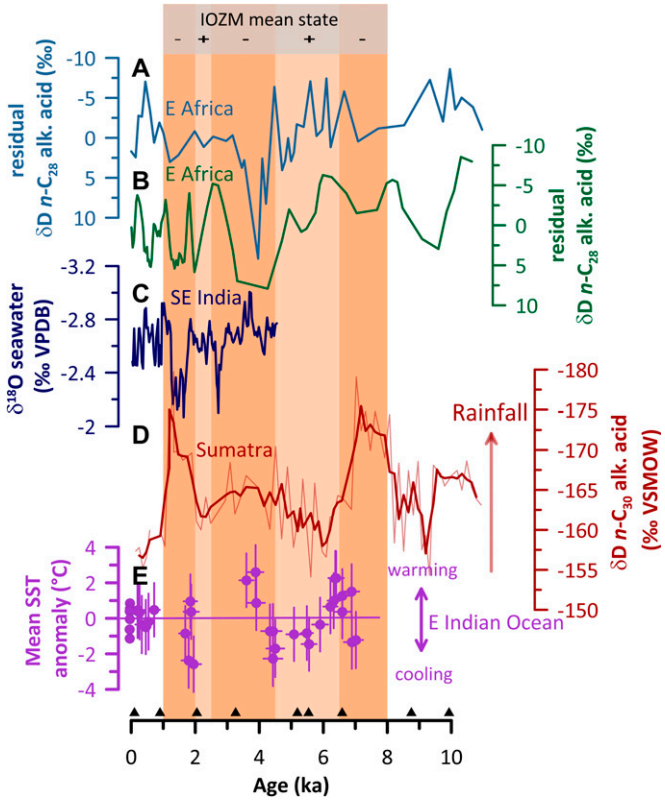

Fig. 3. Holocene fluctuations of the Indian Ocean Precipitation Dipole. (*A* and *B*) Plant wax δD records from the Gulf of Aden (*A*) and Lake Challa (*B*), East Africa (34, 35). Both records were high-pass filtered to illustrate precipitation changes superimposed on long-term monsoonal forcing. (*C*) $\delta^{18}O$ of *Globigerinoides ruber* corrected for ice volume effects as proxy for monsoon intensity in Southeast India (37). (*D*) δD record of the *n*-C_{30} alkanoic acid (this study). (*E*) Eastern Indian Ocean SST anomaly recorded in corals from the Mentawai Islands (6) off western Sumatra. *B, C,* and *D* are plotted as three-point running mean. Black triangles indicate ^{14}C age control points of core SO189-144KL (38). VPDB, Vienna Pee Dee Belemnite; VSMOW, Vienna standard mean ocean water.

Summary and Conclusions. Our study shows that glacial–interglacial changes in sea level and ITCZ position were of minor importance for hydroclimate development in the western IPWP during the past 24 ka, in contrast to the interior of the Maritime Continent. The regionally different records of terrestrial precipitation across the IPWP now allow us to resolve a heterogeneous pattern of deglacial climate change reflecting the glacial continentality of the various sites. Moreover, we find that fluctuations of the Indian Ocean precipitation dipole have been a recurrent if not persistent feature throughout the Holocene and suggest changes of the coupled ocean–atmosphere system over the Indian Ocean, the IOZM, as the underlying cause. Whether our plant wax δD record reflects changes in the frequency of individual positive and negative IOZM events, or swings of the mean state of the IOZM, however, remains unanswered as our integrated plant wax δD signal does not resolve seasonal characteristics of precipitation. High-resolution proxy records of both Indian Ocean conditions and precipitation changes on the surrounding continents are therefore required to further elucidate past dynamics and mechanistic control of the IOZM on western IPWP hydrology.

Materials and Methods

Marine sediment core SO189-144KL was retrieved from the Nias basin off NW Sumatra (western IPWP, 1°09.300 N; 98°03.960 E) at 481 m water depth (Fig. 1) during RV *Sonne* cruise 189-2 in 2006. Core chronology (38) indicates an age of 140 y before present (yr BP) at the top and of 23.9 thousand yr BP (ka) at the bottom, and an average temporal resolution of about 30 y per sample.

Sediments were extracted using a MARS Xpress microwave extraction system from CEM GmbH using a mixture of dichloromethane and methanol (9:1). Total lipid extracts were saponified in 1 M $NaOH_{aq}$ at 80 °C for 3 h. Neutral lipids were extracted with hexane; alkanoic acids were extracted at pH 2 with methyl *t*-butyl ether. Alkanoic acids were methylated using BF_3MeOH of known δD and $\delta^{13}C$ values and purified using silica column chromatography followed by $AgNO_3$-coated silica column chromatography. Lipid extraction is detailed in *SI Text*.

Hydrogen isotopic compositions of alkanoic acid methyl esters were measured on a Thermo Trace GC^{ULTRA} coupled to a Finnigan $Delta^{+}XP$ isotope ratio mass spectrometer (IRMS) via a pyrolysis furnace operated at 1430 °C. Isotope values were calibrated against an H_2 reference gas together with a coinjected *n*-C_{36} alkane standard. δD values of alkanoic acid methyl esters were corrected for additional hydrogen introduced during methylation and are reported in ‰ relative to Vienna standard mean ocean water.

Stable carbon isotopic compositions of alkanoic acid methyl esters were measured on a Thermo Trace GC coupled to a Delta V^{+} IRMS via a combustion furnace operated at 1030 °C. Isotope values were calibrated against a CO_2 reference gas and are reported in ‰ relative to Vienna Pee Dee Belemnite. Details of isotope analyses are provided in *SI Text*.

ACKNOWLEDGMENTS. We thank Camille Risi for helpful discussions on isotope fractionation of tropical rainfall. We thank Mengfan Zhu for providing the Matlab code used to plot vector winds of Fig. S1, and Matthew Forrest for helping us to create Fig. S2. Lichun Zhang and Miguel Rincon are acknowledged for laboratory assistance. This study used samples acquired during cruise SO189-2 in September 2006 through the Federal Institute for Geoscience and Natural Resources (BGR) Hannover, Germany, kindly provided by Andreas Lückge (BGR). Financial support for this research was provided by the Caltech Foster and Coco Stanback fellowship and the research funding programme "LOEWE – Landes-Offensive zur Entwicklung Wissenschaftlich-ökonomischer Exzellenz" of Hesse's Ministry of Higher Education, Research, and the Arts to E.M.N., U.S. National Science Foundation Award 1002656 to S.J.F., and Deutsche Forschungsgemeinschaft Grant HE 3412/15-1 to M.M.

1. Saji NH, Goswami BN, Vinayachandran PN, Yamagata T (1999) A dipole mode in the tropical Indian Ocean. *Nature* 401(6751):360–363.
2. Webster PJ, Moore AM, Loschnigg JP, Leben RR (1999) Coupled ocean-atmosphere dynamics in the Indian Ocean during 1997-98. *Nature* 401(6751):356–360.
3. Aldrian E, Susanto RD (2003) Identification of three dominant rainfall regions within Indonesia and their relationship to sea surface temperature. *Int J Climatol* 23(12): 1435–1452.
4. Tierney JE, Smerdon JE, Anchukaitis KJ, Seager R (2013) Multidecadal variability in East African hydroclimate controlled by the Indian Ocean. *Nature* 493(7432):389–392.
5. Abram NJ, et al. (2007) Seasonal characteristics of the Indian Ocean Dipole during the Holocene epoch. *Nature* 445(7125):299–302.
6. Abram NJ, McGregor HV, Gagan MK, Hantoro WS, Suwargadi BW (2009) Oscillations in the southern extent of the Indo-Pacific Warm Pool during the mid-Holocene. *Quat Sci Rev* 28(25-26):2794–2803.
7. Behera SK, et al. (2006) A CGCM Study on the interaction between IOD and ENSO. *J Clim* 19(9):1688–1705.
8. Murtugudde R, McCreary JP, Busalacchi AJ (2000) Oceanic processes associated with anomalous events in the Indian Ocean with relevance to 1997–1998. *J Geophys Res* 105(C2):3295–3306.
9. Fontanel J, Chantefort A (1978) *Bioclimats du monde Indonésien*, ed Legris P [*Bioclimates of the Indonesian Archipelago*] (Inst Francais Pondichéry, Pondicherry). French.
10. Luo J-J, et al. (2010) Interaction between El Niño and extreme Indian Ocean dipole. *J Clim* 23(3):726–742.
11. Gingele FX, De Deckker P, Hillenbrand C-D (2001) Clay mineral distribution in surface sediments between Indonesia and NW Australia — source and transport by ocean currents. *Mar Geol* 179(3-4):135–146.
12. Ehlert C, et al. (2011) Current transport versus continental inputs in the eastern Indian Ocean: Radiogenic isotope signatures of clay size sediments. *Geochem Geophys Geosyst* 12(6):Q06017, 10.1029/2011GC003544.
13. Sachse D, et al. (2012) Molecular paleohydrology: Interpreting the hydrogen-isotopic composition of lipid biomarkers from photosynthesizing organisms. *Annu Rev Earth Planet Sci* 40(1):221–249.
14. Dansgaard W (1964) Stable isotopes in precipitation. *Tellus* 16(4):436–468.
15. Maloney BK (1980) Pollen analytical evidence for early forest clearance in North Sumatra. *Nature* 287(5780):324–326.
16. Morley RJ (1982) A palaeoecological interpretation of a 10,000 year pollen record from Danau Padang, Central Sumatra, Indonesia. *J Biogeogr* 9(2):151–190.
17. Newsome J, Flenley JR (1988) Late Quaternary vegetational history of the central highlands of Sumatra. II. Palaeopalynology and vegetational history. *J Biogeogr* 15(4): 555–578.
18. Lückge A, et al. (2009) Monsoon versus ocean circulation controls on paleoenvironmental conditions off southern Sumatra during the past 300,000 years. *Paleoceanography* 24(1):PA1208, 10.1029/2008PA001627.
19. Mohtadi M, et al. (2010) Late Pleistocene surface and thermocline conditions of the eastern tropical Indian Ocean. *Quat Sci Rev* 29(7-8):887–896.
20. Stuijts I, Newsome JC, Flenley JR (1988) Evidence for late Quaternary vegetational change in the Sumatran and Javan highlands. *Rev Palaeobot Palynol* 55(1-3):207–216.
21. Shackleton NJ (2000) The 100,000-year ice-age cycle identified and found to lag temperature, carbon dioxide, and orbital eccentricity. *Science* 289(5486):1897–1902.
22. Risi C, Bony S, Vimeux F, Jouzel J (2010) Water-stable isotopes in the LMDZ4 general circulation model: Model evaluation for present-day and past climates and applications to climatic interpretations of tropical isotopic records. *J Geophys Res* 115(D12): D12118, 10.1029/2009JD013255.
23. van der Kaars S, Bassinot F, De Deckker P, Guichard F (2010) Changes in monsoon and ocean circulation and the vegetation cover of southwest Sumatra through the last 83,000 years: The record from marine core BAR94-42. *Palaeogeogr Palaeoclimatol Palaeoecol* 296(1-2):52–78.
24. Partin JW, Cobb KM, Adkins JF, Clark B, Fernandez DP (2007) Millennial-scale trends in west Pacific warm pool hydrology since the Last Glacial Maximum. *Nature* 449(7161): 452–455.
25. Griffiths ML, et al. (2009) Increasing Australian-Indonesian monsoon rainfall linked to early Holocene sea-level rise. *Nat Geosci* 2(9):636–639.
26. Tierney JE, et al. (2012) The influence of Indian Ocean atmospheric circulation on Warm Pool hydroclimate during the Holocene epoch. *J Geophys Res* 117(D19): D19108, 10.1029/2012JD018060.
27. Hanebuth T, Stattegger K, Grootes PM (2000) Rapid flooding of the Sunda Shelf: A late-glacial sea-level record. *Science* 288(5468):1033–1035.
28. Nishimura S, et al. (1984) A gravity and volcanostratigraphic interpretation of the Lake Toba region, North Sumatra, Indonesia. *Tectonophysics* 109(3-4):253–272.
29. Nitta T, Mizuno T, Takahashi K (1992) Multi-scale convective systems during the initial phase of the 1986/87 El Niño. *J Meteorol Soc Jpn* 70(1B):447–466.
30. Mohtadi M, et al. (2011) Glacial to Holocene swings of the Australian-Indonesian monsoon. *Nat Geosci* 4(8):540–544.
31. Rybicki GB, Press WH (1995) Class of fast methods for processing irregularly sampled or otherwise inhomogeneous one-dimensional data. *Phys Rev Lett* 74(7):1060–1063.
32. Davis JC (1986) *Statistics and Data Analysis in Geology* (Wiley, New York).
33. Sinninghe Damsté JS, et al. (2011) A 25,000-year record of climate-induced changes in lowland vegetation of eastern equatorial Africa revealed by the stable carbon-isotopic composition of fossil plant leaf waxes. *Earth Planet Sci Lett* 302(1-2):236–246.
34. Tierney JE, Russell JM, Sinninghe Damsté JS, Huang Y, Verschuren D (2011) Late Quaternary behavior of the East African monsoon and the importance of the Congo Air Boundary. *Quat Sci Rev* 30(7-8):798–807.
35. Tierney JE, deMenocal PB (2013) Abrupt shifts in Horn of Africa hydroclimate since the Last Glacial Maximum. *Science* 342(6160):843–846.
36. Koutavas A, Lynch-Stieglitz J, Marchitto TM, Jr., Sachs JP (2002) El Niño-like pattern in ice age tropical Pacific sea surface temperature. *Science* 297(5579):226–230.
37. Ponton C, et al. (2012) Holocene aridification of India. *Geophys Res Lett* 39(3):L03704, 10.1029/2011GL050722.
38. Mohtadi M, et al. (2014) North Atlantic forcing of tropical Indian Ocean climate. *Nature* 509(7498):76–80.